Article

Wet-Process-Modified Blue-Green Algae Biochar by K$_2$FeO$_4$ for the Efficient Adsorption of Cr(VI) from Water

Aihua Cheng [1], Xingwen Wang [1], Xiaohe Liu [1,*] and Chi He [2]

[1]   School of Geology and Environment, Xi'an University of Science and Technology, Xi'an 710049, China
[2]   School of Energy and Power Engineering, Xi'an Jiaotong University, Xi'an 710049, China
*   Correspondence: xiaohe-liu@outlook.com

Abstract: Iron-modified biochar adsorbent shows its promise for removing Cr(VI) from water. However, the traditional dry-grinding modification methods to prepare iron-modified biochar (DFeBC) usually result in the aggregation of iron oxide particles, thus impeding the adsorption capacity. Herein, blue-green algae waste derived biochar modified in a wet process by K$_2$FeO$_4$ (WFeBC) was developed, and it showed well-distributed iron oxide on the surface of the biochar. As a result, WFeBC displayed a larger theoretical adsorption capacity of 66.22 mg/g than that of DFeBC (48.54 mg/g). It was found that the uniform-distributed iron oxide and abundant oxygen functional groups of WFeBC played an important role in the removal process of Cr(VI). In the adsorption process, the reduction of Cr(VI) to Cr(III) by Fe(II) promoted the removal of hexavalent chromium. The Cr(VI) will be attracted by protonated oxygen functional groups through electrostatic interaction and complexation in an acid environment. All the results show that the wet modification of biochar by K$_2$FeO$_4$ can effectively improve the removal ability of WFeBC to Cr(VI).

Keywords: blue-green algae; adsorption; hexavalent chromium; potassium ferrite; wet modification

1. Introduction

Chromium is mainly contained in the industrial wastewater of electroplating, medicine, chemical fertilizer, printing, and dyeing, mainly in the forms of Cr(III) and Cr(VI). Among them, Cr(VI) has higher soil fluidity and toxicity [1,2], and it can easily dissolve and diffuse in tissues and enter cells through non-specific anion channels [3,4]. Chromium has many toxic effects, such as respiratory problems, hemolysis, acute renal failure, weakened immune system, genetic material changes, lung cancer, and pulmonary fibrosis [4,5]. The permissible limit for chromium is 0.05 mg/L, as recommended by the World Health Organization (WHO). The United States Environmental Protection Agency (USEPA) sets the maximum allowable limit of chromium in drinking water as 0.015 mg/L [6].

At present, the main technologies for Cr(VI) removal include membrane separation, ion exchange, chemical precipitation, electrodialysis, electrocoagulation, adsorption, etc. [7]. The advantages and disadvantages of the main technologies for Cr(VI) removal are shown in the Supplementary Materials (Table S1). These methods have a good treatment effect on hexavalent chromium. However, at the same time, various treatment methods still have some inherent shortcomings, such as secondary pollution, high dependence on materials, membrane aperture and composition, high dependence on resin structure and solution environment, poor system reactor design and electrode sacrifice, dependence on electrode materials and electrochemical surface area, high electrode cost, and unnecessary by-products [8]. Therefore, adsorption methods with advantages such as a high removal rate, low cost, abundant raw materials, and no secondary pollution have attracted wide attention [9–12].

The key to adsorption methods is the adsorbent materials with high adsorbable capacity. Currently, biochar has attracted much attention due to its advantages such as

a wide source of materials, a low cost, a simple preparation method, and being non-toxic [13]. However, the adsorption capacity of pure biochar is limited, so it needs to be modified to increase the surface functional groups or improve the pore structure. In a study on the adsorption of anions, iron oxides show certain adsorption effects on anions. In addition, iron-modified biochar can be separated from aqueous solution due to its good magnetism [14]. Previous studies have shown that modification of biochar by using iron oxide can enhance the removal ability of Cr(VI) in an aqueous solution [15]. However, the traditional modification methods will cause some iron oxide particles to gather in the voids or surfaces of biochar and occupy some active sites, affecting its removal effect on Cr(VI) in solution [16,17]. This indicated that the removal ability of Cr(VI) in the solution can be further improved by improving the modification method of the adsorbent.

Potassium ferrite (K_2FeO_4) is a kind of iron salt with a strong oxidation ability. Its oxidation ability is stronger than potassium permanganate, and it is soluble in water to decompose into KOH. Acid–base modification or oxidation modification can increase the specific surface area, the number and type of surface functional groups, the ion exchange capacity, and other properties of biochar. Introducing transition metals or their oxides into the biochar matrix to form magnetic biochar makes it easier to separate biochar from solution. Therefore, K_2FeO_4, which has the functions of oxidative activation, ferric oxide loading, and KOH activation, is an excellent modifier. It is known that there are few studies using K_2FeO_4-modified biochar, and most of them are based on the traditional grinding method. In order to further improve the adsorption capacity of modified biochar and reduce the accumulation of iron particles on the surface, wet iron-modified biochar (WFeBC) was prepared using blue-green algae waste as the raw material. At the same time, dry iron-modified biochar (DFeBC) was prepared by the traditional grinding method, and its structural changes were compared and analyzed to study the removal ability of Cr(VI) in water. The results showed that the iron oxide was more uniformly distributed on the surface of biochar and the oxidation of biochar was more sufficient by wet process modification. This study promoted the modification of biochar materials in a certain sense and provided theoretical support for the removal of Cr(VI) in an aqueous solution.

In summary, the composite or modification of materials plays a very important role in improving the properties [18–20], and different modification methods have different effects on the performance of biochar. This paper intends to use K_2FeO_4 to modify biochar, and considering the effect of modification methods, we respectively use wet and dry to prepare modified biochar. The morphologies and physicochemical properties of different carbon materials were characterized, and the best modification method was obtained by combining with the study of Cr(VI) adsorption properties, which provided a new idea for the modification of biochar.

2. Materials and Methods

2.1. Materials

Blue-green algae, mostly microcystis, was collected from a pond at the Lintong Campus of Xi'an University of Science and Technology in Shaanxi, China. All chemicals used in this study, such as potassium ferrite (K_2FeO_4), potassium dichromate ($K_2Cr_2O_7$), sodium hydroxide (NaOH), and hydrochloric acid (HCl), are of analytical grade; therefore, they were used directly without further purification. The hexavalent chromium solution (100 mg/L) was prepared by dissolving 0.2829 g $K_2Cr_2O_7$ in 1 L deionized water, which was then diluted to the desired concentration. The pH required for the Cr(VI)solution was adjusted by NaOH and HCl solution with fixed concentration.

2.2. Biochar Preparation

The preparation process of materials is shown in Figure S1 of the Supplementary Materials. The blue-green algae collected in the pond were cleaned with deionized water, dried in a 60 °C oven, crushed and passed through a 60-mesh screen to obtain dried blue-green algae powder, and set aside. Dried blue-green algae powder was mixed with

potassium ferrite in a 5:1 ratio; then, 10 mL of deionized water was added and stirred for 12 h. The evenly stirred suspension was collected and dried in the oven at 60 °C, and then the mixture was heated in a nitrogen tube furnace at a heating rate of 5 °C/min to 300 °C and heated at this temperature for 1 h. The biochar obtained was cleaned with deionized water until colorless and dried at 60 °C. After the above work, the modified biochar (WFeBC) with the improved modification method was obtained and the yield of WFeBC was about 77.8%. In addition, dry modified biochar was prepared according to the previously reported process [10], the dry blue-green algae powder was mixed with potassium ferrite at the ratio of 5:1 (g/g), and directly ground for a certain time without adding water, then pyrolysis was performed. The subsequent operation was consistent with that of WFeBC, and dry modified biochar (DFeBC) was obtained by grinding and modifying traditional potassium ferrite for a yield of DFeBC that was about 80.6%. Biochar (BC) was directly produced from blue-green algae biochar without potassium ferrate treatment, and the yield of BC was about 73.6%.

2.3. Characterization

The specific surface area of the sample was analyzed and tested by ASAP 2020 automatic physicochemical adsorption apparatus (Micromeritics, Norcross, GA, USA). The micromorphology and element of the samples were characterized and observed by JSM-6700F scanning electron microscope (JEOL Company, Tokyo, Japan) with energy-dispersive X-ray spectroscopy (EDS). Thermogravimetric analysis of the samples was performed by TGA-1000 thermogravimetric analyzer (Shanghai Innuo Precision Instrument Co., Ltd., Shanghai, China). The crystal structure of the sample was further characterized by X-ray diffraction (XRD) with scans at a scan rate of 0.02 per second by D 8 Advance X-ray diffractometer (Bruker, Mannheim, Germany). The surface elemental valence states of the samples before and after Cr adsorption were determined by ESCALAB 250 Xi X-ray photoelectron spectroscopy and Auger electron spectroscopy (Thermo Fisher Scientific, Waltham, MA, USA).

The surface functional groups of the samples were gained by a Fourier transform infrared spectroscopy (FTIR), which scans in the wavenumber of 4000–400 cm^{-1} by Perkinelmer 550s Fourier infrared spectrometer (PerkinElmer Company, Waltham, MA, USA).

2.4. Batch Adsorption Experiments

All adsorption experiments were carried out in 150 mL conical flask and oscillated in a mechanical shaker at a rotational speed of 150 rpm at room temperature (25 °C). Generally, 50 mL of chromium solution with an initial pH of 2 (usually 20 mg/L, unless otherwise noted) and 0.05g adsorbent material (1 g/L) were mixed into flask bottles.

In order to explore the influence of pyrolysis temperature on the adsorption capacity of the material, the experiment was carried out in a chromium solution with an initial concentration of 20 mg/L and adsorbed at 25 °C for 20 h. The experiment was carried out in a chromium solution with an initial concentration of 20 mg/L and adsorbed at 25 °C for 10 h to explore the influence of the ratio of blue-green algae to potassium ferrite on the adsorption capacity of the material.

To explore the influence of the initial pH value of the solution, the experiment was conducted in the initial concentration of 20 mg/L, and the solution pH ranged from 2 to 7 in the chromium solution at 25 °C adsorption for 10 h.

The adsorption kinetics experiment was set up in the initial concentration of 20 mg/L, pH of 2 chromium solution under the condition of 25 °C, with sampling and testing at different time intervals.

Adsorption isotherms and thermodynamic experiments were conducted at different initial concentrations from 5 to 100 mg/L at a certain temperature gradient (25, 35, 45 °C).

All experiments were conducted in parallel to reduce errors in experimental results caused by random events. The adsorption capacity of the sample was determined by the concentration difference of Cr(VI) before and after adsorption. The concentration of Cr(VI)

was determined by diphenylcarbonyl hydrazine colorimetric method at 540 nm wavelength using 722 N UV-vis spectrophotometer (Shanghai Electronics Co., Ltd., Shanghai, China).

3. Results and Discussion

3.1. Characterization

Scanning electron microscopy (SEM) analysis shows in Figure 1 that both WFeBC and DFeBC surfaces were oxidized after potassium ferrite modification. Iron oxide particles were observed on the surface and the pore structure of biochar was modified to become rougher. Compared with DFeBC, WFeBC had irregular and wrinkled surface morphologies after modification [21]. In conclusion, the modified method of using potassium ferrite to modify biochar is more beneficial to surface oxidation and pore structure generation than the traditional grinding method.
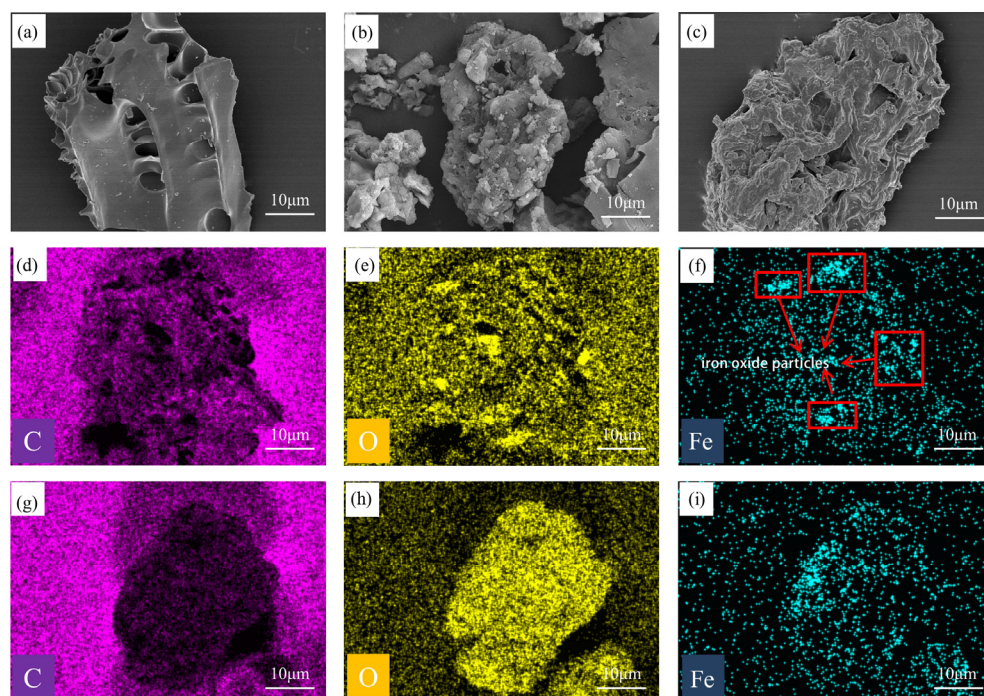

Figure 1. SEM images of BC (**a**), DFeBC (**b**), and WFeBC (**c**) and the EDS mapping of DFeBC (**d–f**) and WFeBC (**g–i**).

According to EDS analysis, Fe on the WFeBC surface is more evenly distributed than that on DFeBC surface. These suggest that the modified method of using potassium ferrite to modify biochar can make the distribution of iron oxide particles on the surface of the material more uniform to increase the exposure of iron oxide particles, so as to promote their interaction with pollutants in water.

The N_2 adsorption–desorption isotherms and pore size distributions of WFeBC, DFeBC, and BC are shown in Figure 2. The isotherms of DFeBC can be divided into type IV isotherms. However, the isotherms of WFeBC and BC belong to type III isotherms, and the adsorption capacity of nitrogen is limited at the saturation pressure point ($P/P_0 = 1$). After modification, the specific surface area of DFeBC and WFeBC is 21.7 m^2/g and 27.9 m^2/g, respectively, and both are higher than the 5.2 m^2/g of BC. This may be because K_2FeO_4 plays a role in promoting oxidation during pyrolysis. This also suggests that the addition of appropriate K_2FeO_4 can avoid the surface area reduction caused by iron and ferrous compounds as precursors in the preparation of magnetic biochar. In addition, the specific surface area of WFeBC is higher than DFeBC, which indicates that the wet modification has a better oxidation effect on the material. The further reduction of the specific surface area is caused by the accumulation of iron and ferrous compounds. At the same time, it

can be seen from the pore size distribution diagram that WFeBC has a more abundant pore structure than BC and DFeBC, and the pore size is mainly concentrated at 5 nm. This is more conducive to the full contact and removal of Cr(VI).
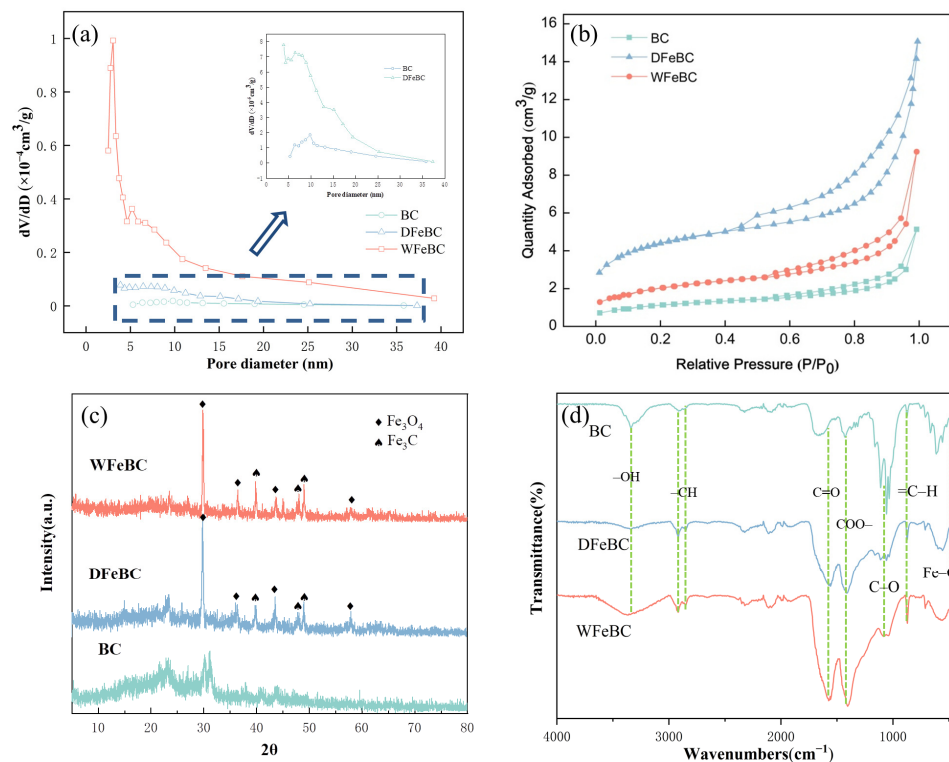

Figure 2. Pore size distributions (**a**), N2 adsorption–desorption isotherms (**b**), XRD patterns (**c**), and FTIR analysis (**d**) of materials.

In order to better study the crystal composition of magnetic biochar, X-ray diffraction was used for the analysis. The XRD spectra of DFeBC, WFeBC, and BC are shown in Figure 2. There was a broad diffraction peak at 2θ = 23.6°, which represented the (002) plane of graphite carbon, demonstrating the existence of highly disordered structures in materials. By comparing the XRD spectra of the materials before and after modification, it can be obviously observed that there are iron particles loaded on the material and that the crystal structure of the two materials is very similar, as both are composed of Fe_3O_4 and Fe_3C crystals. It can be seen that the main magnetic sources of the two modified biochar are Fe_3O_4 and Fe_3C [22]. Both Fe_3O_4 and Fe_3C are produced by the oxidation–reduction of K_2FeO_4 during the thermal decomposition reaction [23]. This is consistent with the morphology of particles on the surface of the modified materials shown by SEM images.

The effect of potassium-ferrite-modified biochar on surface functional groups was further analyzed based on the FTIR spectra (Figure 2). The types of energy hangers of both DFeBC and WFeBC contained were similar including. The peak around 3000–3445 cm^{-1} was attributed to the –OH groups [24]. The peaks at 2925 cm^{-1} and 2858 cm^{-1} were assigned to the –CH_2 groups [25]. The peaks at 1512 cm^{-1} and 1383 cm^{-1} represent C=O stretching vibration of lignin and –COOH groups, respectively [26]. The peaks at 1060 cm^{-1} were assigned to C–O stretching vibrations. The peaks characteristic of Fe–O stretching are located around 475 cm^{-1} [27].

By comparing the biochar before and after potassium ferrite modification, it can be analyzed that the C–O functional groups on the biochar surface are greatly reduced and both WFeBC and DFeBC had more C=O and –COO groups as the asymmetric blending vibration peak of –COOH at 1383 cm^{-1} increased with K_2FeO_4 oxidation [28]. The C=O and –COO groups play an important role in adsorption. Meanwhile, the decrease of

alkaline functional groups and the increase in acidic functional groups on the surface of materials are more beneficial to the adsorption of heavy metal ions. Additionally, compared with DFeBC, WFeBC has more oxygen-containing functional groups, such as C=O and –COO. This shows that the modified method has a better oxidation effect on biochar. In addition, new Fe–O functional groups appeared in the modified material, indicating that Fe was successfully oxidized to the surface of biochar, which is consistent with the previous XRD structure.

3.2. Adsorption of Hexavalent Chromium

3.2.1. Effect of Preparation Parameters

The influence of the pyrolysis temperature of materials on adsorption performance is shown in Figure 3. When the temperature increases from 300 °C to 400 °C or 500 °C, the adsorption performance of materials decreases with the increase in temperature, and materials had the best adsorption performance at 300 °C, which may be due to the decrease in surface functional groups caused by the increase in the temperature of blue-green algae materials. Therefore, 300 °C was chosen as the optimal pyrolysis temperature.
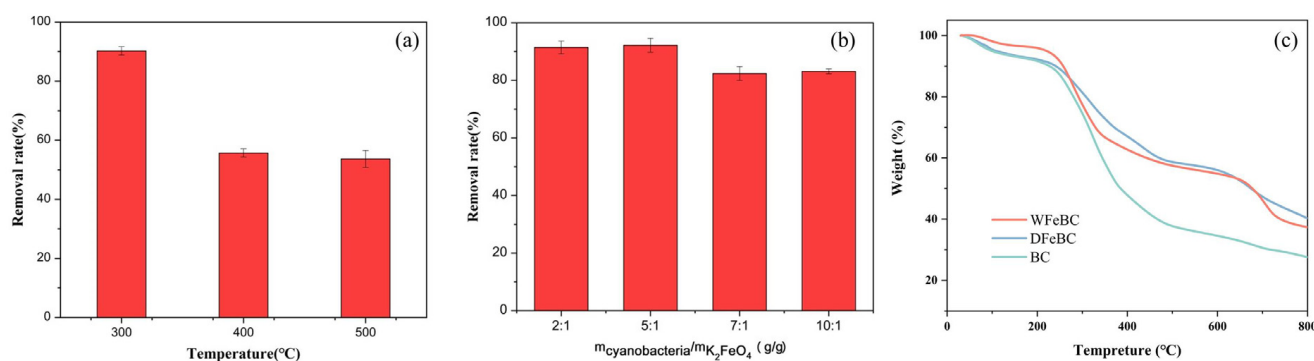

Figure 3. Effect of pyrolysis temperature (**a**) and mixing ratio (**b**) and thermogravimetric analysis of materials (**c**).

The influence of the ratio of blue-green algae to K_2FeO_4 on adsorption performance during the preparation of modified biochar is shown in Figure 3. When the amount of K_2FeO_4 decreases, the adsorption capacity of the material decreases. However, when the ratio of blue-green algae to K_2FeO_4 is 2:1, the adsorption capacity of the material is similar to that when the ratio of blue-green algae to K_2FeO_4 is 5:1. This may be attributed to the fact that ferric oxide particles will also partially aggregate in the pores of biochar, resulting in limited opportunities for contact with pollutants. Therefore, some ferric oxide particles may affect the removal of Cr(VI). Therefore, a 5:1 ratio of blue-green algae to K_2FeO_4 was selected as the optimal preparation condition.

Figure 3c shows the thermogravimetric analysis of materials, which reflects the thermal stability of the materials. For BC, the pyrolysis process can be divided into two parts. The first stage (0–300 °C) is mainly the volatilization of water and some unstable components. The second stage of pyrolysis occurs at 300–500 °C, when volatile compounds, some relatively stable components, and light components of the material are volatilized. The pyrolysis process of modified biochar can be divided into three stages. The first stage (<250 °C) is the evaporation of water in the material. At 300–450 °C, the volatile compounds escape after activation, and finally, the relatively stable components decompose at a high temperature (>500 °C). In the pyrolysis process, the pyrolysis rate of WFeBC is higher and the pyrolysis reaction is more intense, which may be related to the generation of WFeBC containing more active groups [29].

3.2.2. Effect of Initial pH

The pH value of the solution is an important factor affecting the adsorption performance of biochar for Cr(VI). On the one hand, Cr exists in different forms under different pH conditions. On the other hand, as an anion of CrO_4^{2-} exists in solution [30], chromium ions are electronegative. The attraction or repulsion between biochar materials and chromium ions will dominate the adsorption process of the material. Therefore, it is of great significance to explore the adsorption of chromium ions by the pH of a solution [31]. The changes in Zeta potential and adsorption capacity of the three materials with pH values are shown in Figure 4. It can be seen from the figure that the surface potential of the modified material is higher than that of BC and that of WFeBC is significantly increased. When the pH is 2, the pH_{pzc} is found, and the surface of WFeBC contains a large amount of positive charge, which is conducive to the attraction of anions. In addition, the adsorption properties of the three materials are enhanced with the decrease in the pH of the solution, so the adsorption properties of the materials are the best when the pH value is 2. The results showed that the modified method increased the acid functional groups on the surface of WFeBC, which was more favorable for Cr(VI) adsorption.
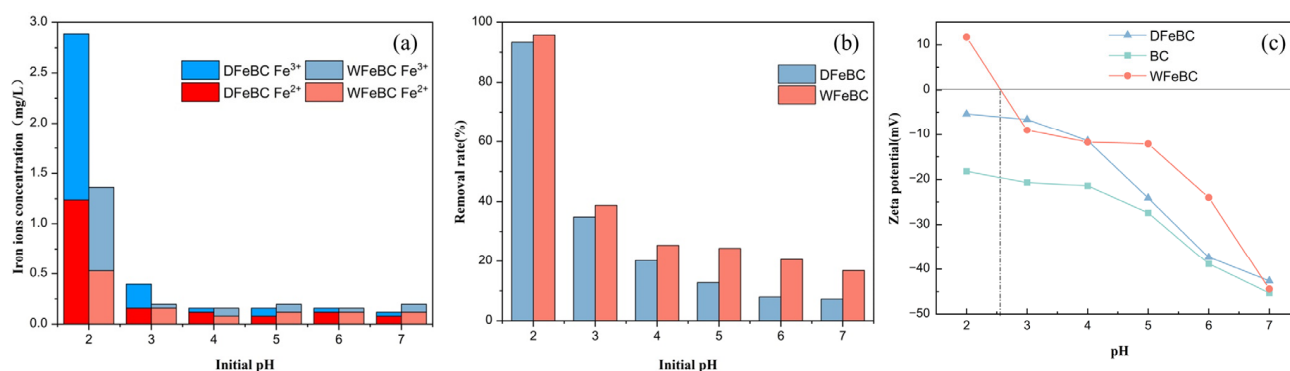

Figure 4. Effect of pH value on iron leaching (**a**), removal rate (**b**), and variation of Zeta potential with pH (**c**).

In the adsorption process, the solution is accompanied by the dissolution of Fe(II) and Fe(III) [32]. The experimental results of the influence of pH value on the leaching concentration of iron ions are shown in Figure 4. With an increase in pH value, the removal effect of the adsorbent decreases, and the concentration of iron ions in the solution, especially Fe(III), decreases obviously. This indicates that the dissolution of iron ions is related to the removal of Cr(VI). It could be that Fe(II) reduces Cr(VI) to Cr(III) dissolved in solution. The experimental results are consistent with the above experiments; when pH = 2, the adsorption effect of the material is the best. In addition, compared with DFeBC, WFeBC has lower iron dissolution, indicating that iron oxides are more stable on the surface of WFeBC materials.

3.3. Kinetics and Isotherms

The curve of material adsorption capacity with time is shown in Figure 5. The adsorption capacity increases with time and reaches adsorption saturation at about 10 h. Through fitting, it is found that the pseudo-second-order adsorption kinetic model has a better fitting effect than the pseudo-first-order adsorption kinetic model. Therefore, the adsorption process of Cr(VI) is more in line with the pseudo-second-order kinetic model, and the adsorption process is mainly chemical adsorption.
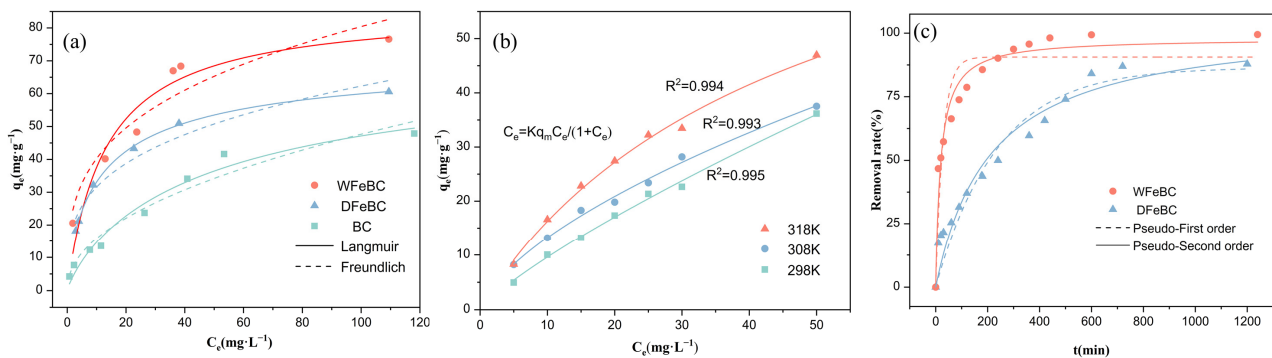
Figure 5. Cr(VI) removal by adsorption isotherm (**a**), adsorption thermodynamics (**b**), and adsorption kinetics (**c**).

The adsorption isotherm experiment results show that WFeBC has a better adsorption effect than DfeBC and that with the increase in adsorption temperature, the adsorption capacity of the material also increases. Moreover, the adsorption of the material is more consistent with the Freundlich isothermal adsorption model, indicating that the adsorption of the material may not be simple monolayer adsorption; that is, the adsorption of the material is non-uniform adsorption on the surface (Table 1). Although the Freundlich model fitted the data slightly better than the Langmuir model, both of them described the isotherm data very well. The constant n fitted by the Freundlich model is within the range of 1–10, indicating that the material is easy to adsorb Cr(VI).

Table 1. The parameters of adsorption isotherm.

Adsorbent	Langmuir Isothermal Adsorption Model			Freundlich Isothermal Adsorption Model		
	b	R^2	Q_m/(mg/g)	K_f	R^2	*n*
DFeBC	0.586	0.877	48.54	18.68	0.9626	3.58
WFeBC	0.228	0.948	66.22	16.81	0.957	2.84

Compared with other materials used for the removal of Cr(VI) in the literature, the Langmuir maximum adsorption capacity of WfeBC has certain advantages (Table 2), and the adsorption equilibrium can be reached faster when combined with the adsorption kinetics data (Table 3).

Table 2. Summary of Cr(VI) adsorption capacity of modified biochar composites in other works.

Materials	pH	Q_e(mg/g)	Reference
BC-Fe-U	2.3–5.7	19.2	[33]
BC@EDTA-LDH	3	38.0	[34]
NMBC	2	48	[35]
Fe/PBC-ND	2	25.68	[36]
Magnetic biochar	1	27.2	[37]
WFeBC	2	66.22	This work.

Table 3. The parameters of adsorption kinetics.

Adsorbent	Pseudo-First-Order Model		Pseudo-Second-Order Model	
	k_1/min^{-1}	R^2	K_2/(g/mg·min)	R^2
DFeBC	0.0023	0.9135	0.0197	0.9567
WFeBC	0.0028	0.6798	0.0027	0.9993

To determine whether the spontaneous adsorption process is the basic condition of the calculation of Gibbs free energy change, ΔG, the adsorption thermodynamics experiment results, as shown in the table from known ΔG < 0, reveal that explanatory material adsorption is spontaneous, and with the absolute value of temperature, ΔG showed a trend of increase, that with the increase in the temperature reaction process, driving force increases. In addition, the experimental ΔH < 0 indicates that the reaction process is endothermic, and rising temperature is conducive to adsorption (Table 4).

Table 4. The parameters of adsorption thermodynamics.

C_0 (mg/L)			298 K	308 K	318 K
	ΔH	ΔS	ΔG	ΔG	ΔG
5	32.0164	0.2004	−27.7129	−29.7173	−31.7216
10	28.5312	0.1849	−26.5651	−28.4140	−30.2628
15	35.2372	0.1894	−21.1994	−23.0932	−24.9871
20	38.4897	0.1997	−21.0290	−23.0263	−25.0236
25	27.9982	0.1581	−19.1227	−20.7040	−22.2852
30	27.0288	0.1539	−18.8211	−20.3597	−21.8983
50	34.7758	0.1767	−17.8850	−19.6521	−21.4193

3.4. Regeneration

The adsorbed saturated material was agitated with 0.1 M NaOH on a shaker at 200 ppm and at room temperature for 12 h, washed and dried, and then put into the adsorption; this was repeated three times [38]. The change in adsorption properties of regenerated biochar is shown in Figure 6. With the increase in regeneration times, the adsorption capacity of the material gradually decreases, which may be caused by incomplete desorption of the material. However, after being repeated three times, the adsorption effect of the material is still 73.37% which indicates that the material has a certain ability to regenerate. Through the analysis of the magnetic regression curve, it can be seen that both modified materials have certain magnetism and that both can be easily separated from aqueous solution under the action of an external magnetic field. The material is stable, easy to recycle, and reusable.
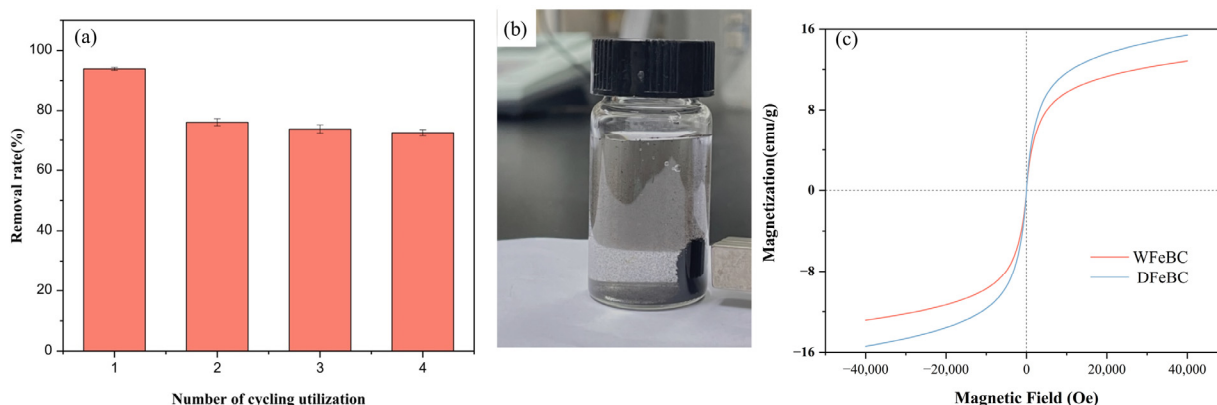

Figure 6. Removal rate of regenerated materials (**a**), magnetic separation image (**b**), and hysteresis loops (HLs) of materials (**c**).

3.5. Adsorption Mechanism

The adsorption mechanism of the material was further analyzed by XPS spectra. The O 1s and C 1s spectras of WFeBC and DFeBC were shown in Figure 7. The functional groups on the surface of the material are consistent with those described by the FTIR analysis and the characteristic peak of Cr appeared after adsorption. The Fe(III) 2p 3/2 peak is located at 711.2 eV, and 724.8 eV corresponds to the 2p 1/2 peak of Fe(III), representing the peak of Fe(II) at 710.9 eV. Compared with the XPS diagram before and after the reaction, the

peak value of Fe(II) decreased from 64.57 to 53.28%, while the content of Fe(III) increased from 35.43 to 46.72% after the reaction. Therefore, it can be understood that part of Fe(II) is converted to Fe(III) in the reduction process of Cr, while Cr(VI) is reduced to Cr(III).
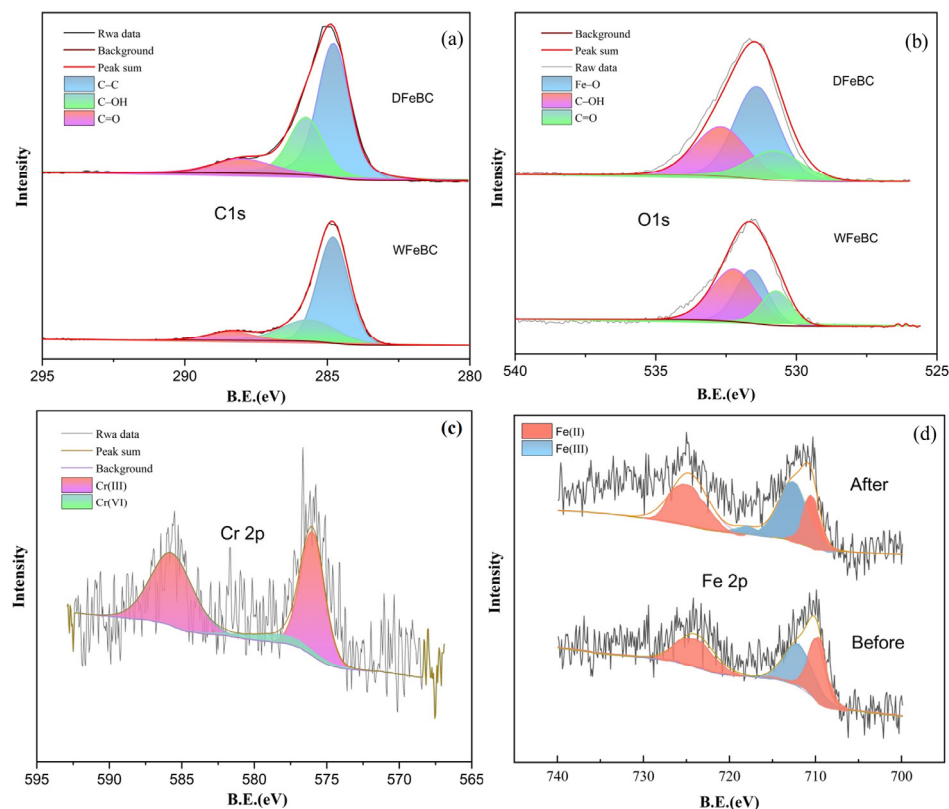

Figure 7. C 1s (**a**) and O 1s (**b**) spectra of DFeBC and WFeBC. Cr 2p spectra of post-adsorption WFeBC (**c**) and Fe 2p spectra of pre- and post-adsorption WFeBC (**d**).

At the same time, by comparing the Cr element on the material surface before and after the reaction, it can be observed that a new Cr element is added to the material surface after the reaction. Combined with the analysis of other experimental characterization data, it can be seen that during the adsorption process of Cr(VI) by blue-green algae modified biochar material, oxidation–reduction reactions occurred between C–O and COOH groups on the material surface and Cr(VI), and oxygen-containing functional groups on the material surface were protonated at pH = 2. Therefore, Cr(VI) in the form of $HCrO_4^-$ can be adsorbed to the surface of biochar materials by electrostatic action. In addition, Cr(III) can occur and precipitate with iron oxides on the material surface and adsorb on the material surface [39]. Compared with the traditional grinding modification method, wet modification makes the surface of biochar more abundant in oxygen-containing functional groups and results in more uniform distribution of iron oxides, so it has a better removal effect.

4. Conclusions

In this study, a magnetic biochar capable of removing Cr(VI) was prepared by using the eutrophic pollutant blue-green algae as a biological template and K_2FeO_4 as a modifier using two modification methods: traditional grinding and wet modification. The results show that, compared with the traditional method, the wet method can oxidize biochar more fully, and the surface of WFeBC has more functional groups and pore structures. Under the condition of 25 °C and pH = 2, the maximum theoretical adsorption capacity can reach 66.22 mg/g. The adsorption process conforms to the quasi-second-order kinetic model and Freundlich isothermal adsorption model. The removal mechanism of Cr(VI)

by the material is shown in Figure 8, including electrostatic adsorption, surface complex precipitation and reduction of iron oxide particles on the material surface.
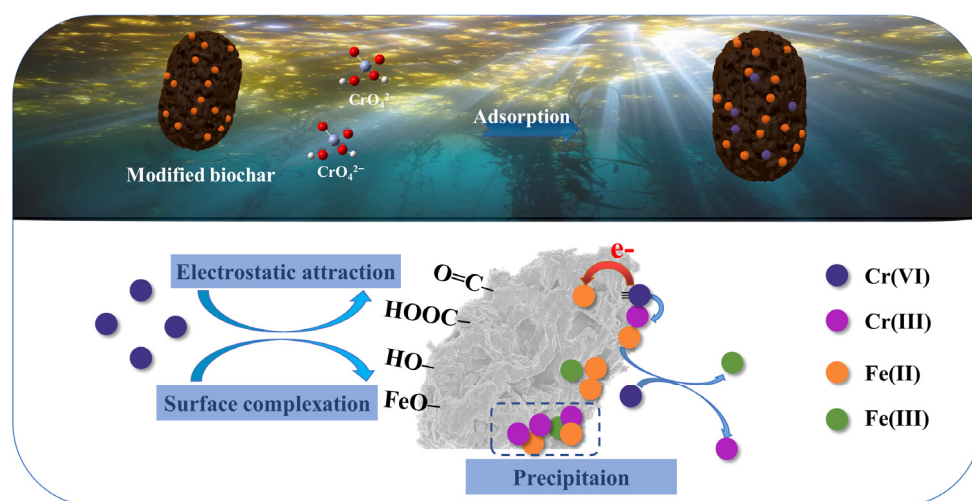

Figure 8. Removal mechanism of Cr(VI) from aqueous solution by K_2FeO_4 modified biochar.

Supplementary Materials: The following supporting information can be downloaded at: https://www.mdpi.com/article/10.3390/pr11051489/s1, Figure S1: The preparation process of materials.; Table S1: The advantages and disadvantages of the main technologies for Cr(VI) removal.

Author Contributions: Conceptualization, A.C. and X.L.; methodology, X.W.; validation, A.C., X.L. and X.W.; formal analysis, X.W.; data curation, X.W.; writing—original draft preparation, X.L. and X.W.; writing—review and editing, X.L. and X.W.; funding acquisition, C.H. All authors have read and agreed to the published version of the manuscript.

Data Availability Statement: All relevant data are within the article.

Conflicts of Interest: The authors declare no conflict of interest.

References

1. Fenti, A.; Chianese, S.; Iovino, P.; Musmarra, D.; Salvestrini, S. Cr(VI) Sorption from Aqueous Solution: A Review. *Appl. Sci.* **2020**, *10*, 6477. [CrossRef]
2. Enniya, I.; Rghioui, L.; Jourani, A. Adsorption of hexavalent chromium in aqueous solution on activated carbon prepared from apple peels. *Sustain. Chem. Pharm.* **2018**, *7*, 9–16. [CrossRef]
3. Tran, H.V.; Tran, T.L.; Le, T.D.; Le, T.D.; Nguyen, H.M.T.; Dang, L.T. Graphene oxide enhanced adsorption capacity of chitosan/magnetite nanocomposite for Cr(VI) removal from aqueous solution. *Mater. Res. Express* **2018**, *6*, 025018. [CrossRef]
4. Mikhaylov, V.I.; Maslennikova, T.P.; Krivoshapkina, E.F.; Tropnikov, E.M.; Krivoshapkin, P.V. Express Al/Fe oxide–oxyhydroxide sorbent systems for Cr(VI) removal from aqueous solutions. *Chem. Eng. J.* **2018**, *350*, 344–355. [CrossRef]
5. Kumar, K.Y.; Muralidhara, H.B.; Nayaka, Y.A.; Balasubramanyam, J.; Hanumanthappa, H. Low-cost synthesis of metal oxide nanoparticles and their application in adsorption of commercial dye and heavy metal ion in aqueous solution. *Powder Technol.* **2013**, *246*, 125–136. [CrossRef]
6. Bagbi, Y.; Sarswat, A.; Mohan, D.; Pandey, A.; Solanki, P.R. Lead and Chromium Adsorption from Water using L-Cysteine Functionalized Magnetite (Fe_3O_4) Nanoparticles. *Sci. Rep.* **2017**, *7*, 7672. [CrossRef]
7. Kerur, S.S.; Bandekar, S.; Hanagadakar, M.S.; Nandi, S.S.; Ratnamala, G.M.; Hegde, P.G. Removal of hexavalent Chromium-Industry treated water and Wastewater: A review. *Mater. Today Proc.* **2021**, *42*, 1112–1121. [CrossRef]
8. Peng, H.; Guo, J. Removal of chromium from wastewater by membrane filtration, chemical precipitation, ion exchange, adsorption electrocoagulation, electrochemical reduction, electrodialysis, electrodeionization, photocatalysis and nanotechnology: A review. *Environ. Chem. Lett.* **2020**, *18*, 2055–2068. [CrossRef]

9. Aryee, A.A.; Dovi, E.; Li, Q.; Han, R.; Li, Z.; Qu, L. Magnetic biocomposite based on peanut husk for adsorption of hexavalent chromium, Congo red and phosphate from solution: Characterization, kinetics, equilibrium, mechanism and antibacterial studies. *Chemosphere* **2022**, *287 Pt 1*, 132030. [CrossRef]

10. Yin, Z.; Xu, S.; Liu, S.; Xu, S.; Li, J.; Zhang, Y. A novel magnetic biochar prepared by K_2FeO_4-promoted oxidative pyrolysis of pomelo peel for adsorption of hexavalent chromium. *Bioresour. Technol.* **2020**, *300*, 122680. [CrossRef]

11. Zou, H.; Zhao, J.; He, F.; Zhong, Z.; Huang, J.; Zheng, Y.; Zhang, Y.; Yang, Y.; Yu, F.; Bashir, M.A.; et al. Ball milling biochar iron oxide composites for the removal of chromium (Cr(VI)) from water: Performance and mechanisms. *J. Hazard. Mater.* **2021**, *413*, 125252. [CrossRef]

12. Yao, X.; Ji, L.; Guo, J.; Ge, S.; Lu, W.; Cai, L.; Wang, Y.; Song, W.; Zhang, H. Magnetic activated biochar nanocomposites derived from wakame and its application in methylene blue adsorption. *Bioresour. Technol.* **2020**, *302*, 122842. [CrossRef]

13. Yang, C.X.; Zhu, Q.; Dong, W.P.; Fan, Y.Q.; Wang, W.L. Preparation and Characterization of Phosphoric Acid-Modified Biochar Nanomaterials with Highly Efficient Adsorption and Photodegradation Ability. *Langmuir* **2021**, *37*, 9253–9263. [CrossRef]

14. Huang, X.; Niu, X.; Zhang, D.; Li, X.; Li, H.; Wang, Z.; Lin, Z.; Fu, M. Fate and mechanistic insights into nanoscale zerovalent iron (nZVI) activation of sludge derived biochar reacted with Cr(VI). *J. Environ. Manag.* **2022**, *319*, 115771. [CrossRef]

15. Zhang, J.; Yu, H.; Xu, W.; Shi, H.; Hu, X.; Xu, J.; Lou, L. Adsorption-reduction coupling mechanism and reductive species during efficient florfenicol removal by modified biochar supported sulfidized nanoscale zerovalent iron. *Environ. Res.* **2023**, *216 Pt 4*, 114782. [CrossRef]

16. Liu, Y.; Shan, H.; Pang, Y.; Zhan, H.; Zeng, C. Iron modified chitosan/coconut shell activated carbon composite beads for Cr(VI) removal from aqueous solution. *Int. J. Biol. Macromol.* **2023**, *224*, 156–169. [CrossRef]

17. Shan, A.; Idrees, A.; Zaman, W.Q.; Abbas, Z.; Ali, M.; Rehman, M.S.U.; Hussain, S.; Danish, M.; Gu, X.; Lyu, S. Synthesis of nZVI-Ni@BC composite as a stable catalyst to activate persulfate: Trichloroethylene degradation and insight mechanism. *J. Environ. Chem. Eng.* **2021**, *9*, 104808. [CrossRef]

18. Ayyob, M.; Bakry, W.M.; Alamier, R.S.; Salama, M.S.; El-Shall, F.S. Awad.Remediation of water containing phosphate using ceria nanoparticles decorated partially reduced graphene oxide (CeO^2-PRGO) composite. *Surf. Interfaces* **2022**, *31*, 102006.

19. Amr, A.; Ibrahim, R.S.; Salama, S.A.; El-Hakam, A.S.; Khder, A.I.A. Synthesis of 12-tungestophosphoric acid supported on Zr/MCM-41 composite with excellent heterogeneous catalyst and promising adsorbent of methylene blue. *Colloids Surf. A Physicochem. Eng. Asp.* **2021**, *631*, 127753.

20. Younes, Y.A.; Kospa, D.A.; Salama, R.S.; Ahmed, A.I.; Ibrahim, A.A. Hydrophilic candle wastes microcapsules as a thermal energy storage material for all-day steam and electricity cogeneration. *Desalination* **2023**, *550*, 116377. [CrossRef]

21. Kim, Y.; Oh, J.-I.; Vithanage, M.; Park, Y.-K.; Lee, J.; Kwon, E.E. Modification of biochar properties using CO_2. *Chem. Eng. J.* **2019**, *372*, 383–389. [CrossRef]

22. Wang, Q.; Zhang, Z.; Xu, G.; Li, G. Magnetic porous biochar with nanostructure surface derived from penicillin fermentation dregs pyrolysis with K_2FeO_4 activation: Characterization and application in penicillin adsorption. *Bioresour. Technol.* **2021**, *327*, 124818. [CrossRef] [PubMed]

23. Xiong, T.; Yuan, X.; Chen, X.; Wu, Z.; Wang, H.; Leng, L.; Wang, H.; Jiang, L.; Zeng, G. Insight into highly efficient removal of cadmium and methylene blue by eco-friendly magnesium silicate-hydrothermal carbon composite. *Appl. Surf. Sci.* **2018**, *427*, 1107–1117. [CrossRef]

24. Leng, L.; Yuan, X.; Zeng, G.; Shao, J.; Chen, X.; Wu, Z.; Wang, H.; Peng, X. Surface characterization of rice husk bio-char produced by liquefaction and application for cationic dye (Malachite green) adsorption. *Fuel* **2015**, *155*, 77–85. [CrossRef]

25. Li, R.; Wang, J.J.; Zhou, B.; Zhang, Z.; Liu, S.; Lei, S.; Xiao, R. Simultaneous capture removal of phosphate, ammonium and organic substances by MgO impregnated biochar and its potential use in swine wastewater treatment. *J. Clean. Prod.* **2017**, *147*, 96–107. [CrossRef]

26. Liu, S.; Li, J.; Xu, S.; Wang, M.; Zhang, Y.; Xue, X. A modified method for enhancing adsorption capability of banana pseudostem biochar towards methylene blue at low temperature. *Bioresour. Technol.* **2019**, *282*, 48–55. [CrossRef]

27. Stoia, M.; Istratie, R.; Păcurariu, C. Investigation of magnetite nanoparticles stability in air by thermal analysis and FTIR spectroscopy. *J. Therm. Anal. Calorim.* **2016**, *125*, 1185–1198. [CrossRef]

28. Zhang, Z.; Huang, G.; Zhang, P.; Shen, J.; Wang, S.; Li, Y. Development of iron-based biochar for enhancing nitrate adsorption: Effects of specific surface area, electrostatic force, and functional groups. *Sci. Total Environ.* **2023**, *856 Pt 1*, 159037. [CrossRef]

29. Yang, Q.; Sun, Y.; Sun, W.; Qin, Z.; Liu, H.; Ma, Y.; Wang, X. Cellulose derived biochar: Preparation, characterization and Benzo[a]pyrene adsorption capacity. *Grain Oil Sci. Technol.* **2021**, *4*, 182–190. [CrossRef]

30. Guo, X.; Liu, A.; Lu, J.; Niu, X.; Jiang, M.; Ma, Y.; Liu, X.; Li, M. Adsorption Mechanism of Hexavalent Chromium on Biochar: Kinetic, Thermodynamic, and Characterization Studies. *ACS Omega* **2020**, *5*, 27323–27331. [CrossRef]

31. Dong, H.; Deng, J.; Xie, Y.; Zhang, C.; Jiang, Z.; Cheng, Y.; Hou, K.; Zeng, G. Stabilization of nanoscale zero-valent iron (nZVI) with modified biochar for Cr(VI) removal from aqueous solution. *J. Hazard. Mater.* **2017**, *332*, 79–86. [CrossRef]

32. He, R.; Yuan, X.; Huang, Z.; Wang, H.; Jiang, L.; Huang, J.; Tan, M.; Li, H. Activated biochar with iron-loading and its application in removing Cr (VI) from aqueous solution. *Colloids Surf. A Physicochem. Eng. Asp.* **2019**, *579*, 123642. [CrossRef]

33. Dobrzyńska, J.; Wysokińska, A.; Olchowski, R. Raspberry stalks-derived biochar, magnetic biochar and urea modified magnetic biochar—Synthesis, characterization and application for As(V) and Cr(VI) removal from river water. *J. Environ. Manag.* **2022**, *316*, 115260. [CrossRef]

34. Huang, D.; Liu, C.; Zhang, C.; Deng, R.; Wang, R.; Xue, W.; Luo, H.; Zeng, G.; Zhang, Q.; Guo, X. Cr(VI) removal from aqueous solution using biochar modified with Mg/Al-layered double hydroxide intercalated with ethylenediaminetetraacetic acid. *Bioresour. Technol.* **2019**, *276*, 127–132. [CrossRef]

35. Wang, F.; Liu, L.-Y.; Liu, F.; Wang, L.-G.; Ouyang, T.; Chang, C.-T. Facile one-step synthesis of magnetically modified biochar with enhanced removal capacity for hexavalent chromium from aqueous solution. *J. Taiwan Inst. Chem. Eng.* **2017**, *81*, 414–418. [CrossRef]

36. Zhang, X.; Lv, L.; Qin, Y.; Xu, M.; Jia, X.; Chen, Z. Removal of aqueous Cr(VI) by a magnetic biochar derived from *Melia azedarach* wood. *Bioresour. Technol.* **2018**, *256*, 1–10. [CrossRef]

37. Shi, S.; Yang, J.; Liang, S.; Li, M.; Gan, Q.; Xiao, K.; Hu, J. Enhanced Cr (VI) removal from acidic solutions using biochar modified by Fe_3O_4@ SiO_2-NH_2 particles. *Sci. Total Environ.* **2018**, *628*, 499–508. [CrossRef]

38. Dong, X.; Ma, L.Q.; Li, Y. Characteristics and mechanisms of hexavalent chromium removal by biochar from sugar beet tailing. *J. Hazard. Mater.* **2011**, *190*, 909–915. [CrossRef]

39. Zhou, Z.; Liu, P.; Wang, S.; Finfrock, Y.Z.; Ye, Z.; Feng, Y.; Li, X. Iron-modified biochar-based bilayer permeable reactive barrier for Cr(VI) removal. *J. Hazard. Mater.* **2022**, *439*, 129636. [CrossRef]